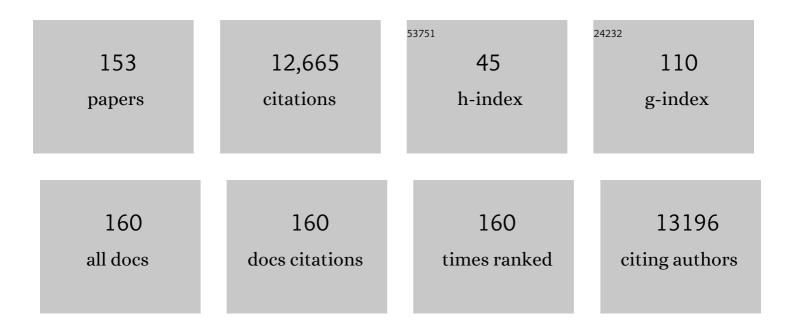
List of Publications by Year in descending order

Source: https://exaly.com/author-pdf/5161345/publications.pdf Version: 2024-02-01



#	Article	IF	CITATIONS
1	Element doping-induced effects in Zn-doped CdTe quantum-dot system: Insights from an ultrafast dynamics perspective. Journal of Chemical Physics, 2022, 156, 034701.	1.2	1
2	Free-standing homochiral 2D monolayers by exfoliation of molecular crystals. Nature, 2022, 602, 606-611.	13.7	60
3	Unraveling the Effect of Surface Ligands on the Auger Process in an Inorganic Perovskite Quantum-Dot System. Journal of Physical Chemistry Letters, 2022, 13, 2943-2949.	2.1	2
4	State-selective exciton–plasmon interplay in a hybrid WSe ₂ /CuFeS ₂ nanosystem. Journal of Chemical Physics, 2022, 156, 144701.	1.2	1
5	A Unique Fe–N ₄ Coordination System Enabling Transformation of Oxygen into Superoxide for Photocatalytic CH Activation with High Efficiency and Selectivity. Advanced Materials, 2022, 34, e2200612.	11.1	43
6	Phononic Fine-Tuning in a Prototype Two-Dimensional Hybrid Organic–Inorganic Perovskite System. Journal of Physical Chemistry Letters, 2022, 13, 5480-5487.	2.1	1
7	A Red-Emitting Cu(I)–Halide Cluster Phosphor with Near-Unity Photoluminescence Efficiency for High-Power wLED Applications. Molecules, 2022, 27, 4441.	1.7	5
8	Forming electron traps deactivates self-assembled crystalline organic nanosheets toward photocatalytic overall water splitting. Science Bulletin, 2021, 66, 265-274.	4.3	18
9	High Quality CsPbl _{3â^'} <i>_x</i> Br <i>_x</i> Thin Films Enabled by Synergetic Regulation of Fluorine Polymers and Amino Acid Molecules for Efficient Pure Red Light Emitting Diodes. Advanced Optical Materials, 2021, 9, 2001684.	3.6	19
10	Site Sensitivity of Interfacial Charge Transfer and Photocatalytic Efficiency in Photocatalysis: Methanol Oxidation on Anatase TiO 2 Nanocrystals. Angewandte Chemie, 2021, 133, 6225-6234.	1.6	7
11	Site Sensitivity of Interfacial Charge Transfer and Photocatalytic Efficiency in Photocatalysis: Methanol Oxidation on Anatase TiO ₂ Nanocrystals. Angewandte Chemie - International Edition, 2021, 60, 6160-6169.	7.2	52
12	A hierarchical heterostructure of CdS QDs confined on 3D ZnIn2S4 with boosted charge transfer for photocatalytic CO2 reduction. Nano Research, 2021, 14, 81-90.	5.8	84
13	Hydrogenated Oxide as Novel Quasi-metallic Cocatalyst for Efficient Visible-Light Driven Photocatalytic Water Splitting. Journal of Physical Chemistry C, 2021, 125, 12672-12681.	1.5	5
14	Negative/Zero Thermal Quenching of Luminescence <i>via</i> Electronic Structural Transition in Copper–lodide Cluster-Based Coordination Networks. Journal of Physical Chemistry Letters, 2021, 12, 8237-8245.	2.1	11
15	Photocatalytic N2 fixation by plasmonic Mo-doped TiO2 semiconductor. Chinese Journal of Chemical Physics, 2021, 34, 413-418.	0.6	Ο
16	Ce-Doped W ₁₈ O ₄₉ Nanowires for Tuning N ₂ Activation toward Direct Nitrate Photosynthesis. Journal of Physical Chemistry Letters, 2021, 12, 11295-11302.	2.1	20
17	High Color Purity and Efficient Green Light-Emitting Diode Using Perovskite Nanocrystals with the Size Overly Exceeding Bohr Exciton Diameter. Journal of the American Chemical Society, 2021, 143, 19928-19937.	6.6	41
18	Efficient infrared light induced CO2 reduction with nearly 100% CO selectivity enabled by metallic CoN porous atomic layers. Nano Energy, 2020, 69, 104421.	8.2	88

#	Article	IF	CITATIONS
19	Increasing Photothermal Efficacy by Simultaneous Intra―and Intermolecular Fluorescence Quenching. Advanced Functional Materials, 2020, 30, 1908073.	7.8	49
20	Structure defects promoted exciton dissociation and carrier separation for enhancing photocatalytic hydrogen evolution. Applied Catalysis B: Environmental, 2020, 264, 118480.	10.8	40
21	Suppressing Auger Recombination in Cesium Lead Bromide Perovskite Nanocrystal Film for Bright Light-Emitting Diodes. Journal of Physical Chemistry Letters, 2020, 11, 9371-9378.	2.1	29
22	Hydrogenâ€Dopingâ€Induced Metalâ€Like Ultrahigh Freeâ€Carrier Concentration in Metalâ€Oxide Material for Giant and Tunable Plasmon Resonance. Advanced Materials, 2020, 32, e2004059.	11.1	57
23	Doping copper ions in a metal-organic framework (UiO-66-NH2): Location effect examined by ultrafast spectroscopy. Chinese Journal of Chemical Physics, 2020, 33, 394-400.	0.6	9
24	Ultraefficient Singlet Oxygen Generation from Manganese-Doped Cesium Lead Chloride Perovskite Quantum Dots. ACS Nano, 2020, 14, 12596-12604.	7.3	20
25	Photoexcited Electron Dynamics of Nitrogen Fixation Catalyzed by Ruthenium Single-Atom Catalysts. Journal of Physical Chemistry Letters, 2020, 11, 9579-9586.	2.1	32
26	Photodissociation dynamics of carbon dioxide cation via the vibrationally mediated A~2Îu,1/2Ï1,Ï2,0/B~2Σu+0,0,0 states in the wavelength range of 282–293Ânm. Chemical Physics Letters, 20 756, 137754.	020,	0
27	Negative thermal quenching of photoluminescence in a copper–organic framework emitter. Chemical Communications, 2020, 56, 12057-12060.	2.2	22
28	Efficient visible light photocatalysis enabled by the interaction between dual cooperative defect sites. Applied Catalysis B: Environmental, 2020, 274, 119099.	10.8	34
29	Ketones as Molecular Coâ€catalysts for Boosting Excitonâ€Based Photocatalytic Molecular Oxygen Activation. Angewandte Chemie - International Edition, 2020, 59, 11093-11100.	7.2	43
30	A Promoted Charge Separation/Transfer System from Cu Single Atoms and C ₃ N ₄ Layers for Efficient Photocatalysis. Advanced Materials, 2020, 32, e2003082.	11.1	333
31	Improving Leadâ€Free Double Perovskite Cs ₂ NaBiCl ₆ Nanocrystal Optical Properties via Ion Doping. Advanced Optical Materials, 2020, 8, 1901919.	3.6	118
32	Amorphous TiO2 as a multifunctional interlayer for boosting the efficiency and stability of the CdS/cobaloxime hybrid system for photocatalytic hydrogen production. Nanoscale, 2020, 12, 11267-11279.	2.8	10
33	Ketones as Molecular Coâ€catalysts for Boosting Excitonâ€Based Photocatalytic Molecular Oxygen Activation. Angewandte Chemie, 2020, 132, 11186-11193.	1.6	9
34	Calcium-tributylphosphine oxide passivation enables the efficiency of pure-blue perovskite light-emitting diode up to 3.3%. Science Bulletin, 2020, 65, 1150-1153.	4.3	39
35	Multi-domain high-resolution platform for integrated spectroscopy and microscopy characterizations. Chinese Journal of Chemical Physics, 2020, 33, 680-685.	0.6	3
36	Impact of structural disorder on excitonic behaviors and dynamics in 2D organic-inorganic hybrid perovskites. Chinese Journal of Chemical Physics, 2020, 33, 561-568.	0.6	0

#	Article	IF	CITATIONS
37	Switching on the Photocatalysis of Metal–Organic Frameworks by Engineering Structural Defects. Angewandte Chemie, 2019, 131, 12303-12307.	1.6	55
38	Switching on the Photocatalysis of Metal–Organic Frameworks by Engineering Structural Defects. Angewandte Chemie - International Edition, 2019, 58, 12175-12179.	7.2	310
39	Metal–Organic Framework Coating Enhances the Performance of Cu ₂ O in Photoelectrochemical CO ₂ Reduction. Journal of the American Chemical Society, 2019, 141, 10924-10929.	6.6	219
40	Rational design of functional materials guided by single particle chemiluminescence imaging. Chemical Science, 2019, 10, 5444-5451.	3.7	18
41	Efficient Exciton Dissociation in Heterojunction Interfaces Realizing Enhanced Photoresponsive Performance. Journal of Physical Chemistry Letters, 2019, 10, 2904-2910.	2.1	26
42	Atomic palladium on graphitic carbon nitride as a hydrogen evolution catalyst under visible light irradiation. Communications Chemistry, 2019, 2, .	2.0	57
43	Photodissociation dynamics of dichlorodifluoromethane (CF2Cl2) around 235 nm using time-sliced velocity map imaging technology. Chinese Journal of Chemical Physics, 2019, 32, 406-410.	0.6	2
44	Energy transfer and electron transfer in composite system of carbon quantum dots/rhodamine B molecules. Chinese Journal of Chemical Physics, 2019, 32, 643-648.	0.6	8
45	Efficient and Color-Tunable Quasi-2D CsPbBr _{<i>x</i>} Cl _{3–<i>x</i>} Perovskite Blue Light-Emitting Diodes. ACS Photonics, 2019, 6, 667-676.	3.2	87
46	Few-Nanometer-Sized α-CsPbl ₃ Quantum Dots Enabled by Strontium Substitution and Iodide Passivation for Efficient Red-Light Emitting Diodes. Journal of the American Chemical Society, 2019, 141, 2069-2079.	6.6	218
47	Experimental Identification of Ultrafast Reverse Hole Transfer at the Interface of the Photoexcited Methanol/Graphitic Carbon Nitride System. Angewandte Chemie - International Edition, 2018, 57, 5320-5324.	7.2	71
48	Graphene Grown on Anatase–TiO ₂ Nanosheets: Enhanced Photocatalytic Activity on Basis of a Well-Controlled Interface. Journal of Physical Chemistry C, 2018, 122, 6388-6396.	1.5	28
49	Experimental Identification of Ultrafast Reverse Hole Transfer at the Interface of the Photoexcited Methanol/Graphitic Carbon Nitride System. Angewandte Chemie, 2018, 130, 5418-5422.	1.6	15
50	Optically Switchable Photocatalysis in Ultrathin Black Phosphorus Nanosheets. Journal of the American Chemical Society, 2018, 140, 3474-3480.	6.6	210
51	Ce ³⁺ -Doping to Modulate Photoluminescence Kinetics for Efficient CsPbBr ₃ Nanocrystals Based Light-Emitting Diodes. Journal of the American Chemical Society, 2018, 140, 3626-3634.	6.6	442
52	Single Pt Atoms Confined into a Metal–Organic Framework for Efficient Photocatalysis. Advanced Materials, 2018, 30, 1705112.	11.1	599
53	Oxygen-Vacancy-Mediated Exciton Dissociation in BiOBr for Boosting Charge-Carrier-Involved Molecular Oxygen Activation. Journal of the American Chemical Society, 2018, 140, 1760-1766.	6.6	651
54	Room temperature precipitated dual phase CsPbBr ₃ –CsPb ₂ Br ₅ nanocrystals for stable perovskite light emitting diodes. Nanoscale, 2018, 10, 19262-19271.	2.8	48

#	Article	IF	CITATIONS
55	Location effect in a photocatalytic hybrid system of metal-organic framework interfaced with semiconductor nanoparticles. Chinese Journal of Chemical Physics, 2018, 31, 613-618.	0.6	12
56	Mechanistic Insights into the Fluorescence Quenching of Rhodamine 6G by Graphene Oxide. Chinese Journal of Chemical Physics, 2018, 31, 165-170.	0.6	8
57	Determining the Chargeâ€Transfer Direction in a p–n Heterojunction BiOCl/gâ€C ₃ N ₄ Photocatalyst by Ultrafast Spectroscopy. ChemPhotoChem, 2017, 1, 350-354.	1.5	18
58	Proton-coupled charge-transfer reactions and photoacidity of N, N -dimethyl-3-arylpropan-1-ammonium chloride salts. Photochemical and Photobiological Sciences, 2017, 16, 972-984.	1.6	6
59	Defect-Mediated Electron–Hole Separation in One-Unit-Cell ZnIn ₂ S ₄ Layers for Boosted Solar-Driven CO ₂ Reduction. Journal of the American Chemical Society, 2017, 139, 7586-7594.	6.6	764
60	Great Disparity in Photoluminesence Quantum Yields of Colloidal CsPbBr ₃ Nanocrystals with Varied Shape: The Effect of Crystal Lattice Strain. Journal of Physical Chemistry Letters, 2017, 8, 3115-3121.	2.1	30
61	Insights into the excitonic processes in polymeric photocatalysts. Chemical Science, 2017, 8, 4087-4092.	3.7	136
62	Interfacially Al-doped ZnO nanowires: greatly enhanced near band edge emission through suppressed electron–phonon coupling and confined optical field. Physical Chemistry Chemical Physics, 2017, 19, 9537-9544.	1.3	5
63	Impact of Element Doping on Photoexcited Electron Dynamics in CdS Nanocrystals. Journal of Physical Chemistry Letters, 2017, 8, 5680-5686.	2.1	20
64	Surface Plasmon Assisted Directional Rayleigh Scattering. Chinese Journal of Chemical Physics, 2017, 30, 135-138.	0.6	10
65	Photodissociation Dynamics of Carbon Dioxide Cation via the Vibrationally Mediated <i>Ã</i> 2Îu,1/2 State: A Time-Sliced Velocity-Mapped Ion Imaging Study. Chinese Journal of Chemical Physics, 2017, 30, 123-127.	0.6	6
66	Boosting Photocatalytic Hydrogen Production of a Metal–Organic Framework Decorated with Platinum Nanoparticles: The Platinum Location Matters. Angewandte Chemie, 2016, 128, 9535-9539.	1.6	122
67	Oxyhydroxide Nanosheets with Highly Efficient Electron–Hole Pair Separation for Hydrogen Evolution. Angewandte Chemie, 2016, 128, 2177-2181.	1.6	26
68	Singleâ€Atom Pt as Coâ€Catalyst for Enhanced Photocatalytic H ₂ Evolution. Advanced Materials, 2016, 28, 2427-2431.	11.1	1,156
69	Oxyhydroxide Nanosheets with Highly Efficient Electron–Hole Pair Separation for Hydrogen Evolution. Angewandte Chemie - International Edition, 2016, 55, 2137-2141.	7.2	99
70	Enhanced Singlet Oxygen Generation in Oxidized Graphitic Carbon Nitride for Organic Synthesis. Advanced Materials, 2016, 28, 6940-6945.	11.1	397
71	Boosting Photocatalytic Hydrogen Production of a Metal–Organic Framework Decorated with Platinum Nanoparticles: The Platinum Location Matters. Angewandte Chemie - International Edition, 2016, 55, 9389-9393.	7.2	513
72	Enhanced Photoexcited Carrier Separation in Oxygenâ€Doped ZnIn ₂ S ₄ Nanosheets for Hydrogen Evolution. Angewandte Chemie - International Edition, 2016, 55, 6716-6720.	7.2	454

#	Article	IF	CITATIONS
73	Probing the ultrafast dynamics in nanomaterial complex systems by femtosecond transient absorption spectroscopy. High Power Laser Science and Engineering, 2016, 4, .	2.0	26
74	Unraveling Surface Plasmon Decay in Core–Shell Nanostructures toward Broadband Light-Driven Catalytic Organic Synthesis. Journal of the American Chemical Society, 2016, 138, 6822-6828.	6.6	136
75	Inâ€situ Integration of a Metallic 1Tâ€MoS ₂ /CdS Heterostructure as a Means to Promote Visibleâ€Lightâ€Driven Photocatalytic Hydrogen Evolution. ChemCatChem, 2016, 8, 2614-2619.	1.8	98
76	Retrieving the Rate of Reverse Intersystem Crossing from Ultrafast Spectroscopy. Journal of Physical Chemistry Letters, 2016, 7, 3908-3912.	2.1	10
77	Enhanced Photoexcited Carrier Separation in Oxygenâ€Doped ZnIn ₂ S ₄ Nanosheets for Hydrogen Evolution. Angewandte Chemie, 2016, 128, 6828-6832.	1.6	42
78	Insight into Electrocatalysts as Co-catalysts in Efficient Photocatalytic Hydrogen Evolution. ACS Catalysis, 2016, 6, 4253-4257.	5.5	120
79	A New Cubic Phase for a NaYF ₄ Host Matrix Offering High Upconversion Luminescence Efficiency. Advanced Materials, 2015, 27, 5528-5533.	11.1	94
80	A Unique Ternary Semiconductor–(Semiconductor/Metal) Nanoâ€Architecture for Efficient Photocatalytic Hydrogen Evolution. Angewandte Chemie - International Edition, 2015, 54, 11495-11500.	7.2	118
81	Atomicâ€Layerâ€Confined Doping for Atomicâ€Level Insights into Visibleâ€Light Water Splitting. Angewandte Chemie - International Edition, 2015, 54, 9266-9270.	7.2	158
82	Rupturing C60Molecules into Graphene-Oxide-like Quantum Dots: Structure, Photoluminescence, and Catalytic Application. Small, 2015, 11, 5296-5304.	5.2	39
83	Efficient and tunable fluorescence energy transfer via long-lived polymer excitons. Polymer Chemistry, 2015, 6, 1698-1702.	1.9	7
84	The laser-induced fluorescence spectroscopy of yttrium monosulfide. Journal of Molecular Spectroscopy, 2015, 313, 49-53.	0.4	1
85	Visible-Light Photoexcited Electron Dynamics of Scandium Endohedral Metallofullerenes: The Cage Symmetry and Substituent Effects. Journal of the American Chemical Society, 2015, 137, 8769-8774.	6.6	29
86	Steering charge kinetics in photocatalysis: intersection of materials syntheses, characterization techniques and theoretical simulations. Chemical Society Reviews, 2015, 44, 2893-2939.	18.7	955
87	Bringing light into the dark triplet space of molecular systems. Physical Chemistry Chemical Physics, 2015, 17, 13129-13136.	1.3	8
88	Molecular co-catalyst accelerating hole transfer for enhanced photocatalytic H2 evolution. Nature Communications, 2015, 6, 8647.	5.8	172
89	Visible-Light Photoreduction of CO ₂ in a Metal–Organic Framework: Boosting Electron–Hole Separation via Electron Trap States. Journal of the American Chemical Society, 2015, 137, 13440-13443.	6.6	927
90	Remarkable enhancement of photovoltaic performance of ZnO/CdTe core–shell nanorod array solar cells through interface passivation with a TiO2 layer. RSC Advances, 2015, 5, 71883-71889.	1.7	10

#	Article	IF	CITATIONS
91	Polymerization-Enhanced Intersystem Crossing: New Strategy to Achieve Long-Lived Excitons. Macromolecular Rapid Communications, 2015, 36, 298-303.	2.0	59
92	Ion-Velocity Map Imaging Study of Photodissociation Dynamics of Acetaldehyde. Chinese Journal of Chemical Physics, 2014, 27, 249-255.	0.6	4
93	Metal–Organic Frameworks: Integration of an Inorganic Semiconductor with a Metal–Organic Framework: A Platform for Enhanced Gaseous Photocatalytic Reactions (Adv. Mater. 28/2014). Advanced Materials, 2014, 26, 4907-4907.	11.1	3
94	Fluorescent switch for fast and selective detection of mercury (II) ions in vitro and in living cells and a simple device for its removal. Talanta, 2014, 125, 204-209.	2.9	16
95	Designing pâ€Type Semiconductor–Metal Hybrid Structures for Improved Photocatalysis. Angewandte Chemie - International Edition, 2014, 53, 5107-5111.	7.2	176
96	Improving the photovoltaic performance of solid-state ZnO/CdTe core–shell nanorod array solar cells using a thin CdS interfacial layer. Journal of Materials Chemistry A, 2014, 2, 5675-5681.	5.2	34
97	Semiconductors: A Unique Semiconductor-Metal-Graphene Stack Design to Harness Charge Flow for Photocatalysis (Adv. Mater. 32/2014). Advanced Materials, 2014, 26, 5578-5578.	11.1	4
98	Integration of an Inorganic Semiconductor with a Metal–Organic Framework: A Platform for Enhanced Gaseous Photocatalytic Reactions. Advanced Materials, 2014, 26, 4783-4788.	11.1	380
99	A Unique Semiconductor–Metal–Graphene Stack Design to Harness Charge Flow for Photocatalysis. Advanced Materials, 2014, 26, 5689-5695.	11.1	134
100	Tunable Oxygen Activation for Catalytic Organic Oxidation: Schottky Junction versus Plasmonic Effects. Angewandte Chemie - International Edition, 2014, 53, 3205-3209.	7.2	136
101	Temperature Dependence of C ₂ (a ³ ĐŸ <sub&g Radical Reactions with Sulfur Bearing Molecules. Wuli Huaxue Xuebao/ Acta Physico - Chimica Sinica, 2014, 30, 797-802.</sub&g 	;t;u <td>&g';)</td>	&g ';)
102	The Realistic Domain Structure of As-Synthesized Graphene Oxide from Ultrafast Spectroscopy. Journal of the American Chemical Society, 2013, 135, 12468-12474.	6.6	64
103	Photodissociation Dynamics of Carbonyl Sulfide in Helium Droplets. Wuli Huaxue Xuebao/ Acta Physico - Chimica Sinica, 2013, 29, 1886-1890.	2.2	0
104	Note: Vibrationally mediated photodissociation of carbon dioxide cation. Journal of Chemical Physics, 2013, 139, 166101.	1.2	7
105	How Graphene Oxide Quenches Fluorescence of Rhodamine 6G. Chinese Journal of Chemical Physics, 2013, 26, 252-258.	0.6	16
106	Helium Droplets: An Apparatus to Study Ultra Cold Chemistry. Chinese Journal of Chemical Physics, 2013, 26, 270-276.	0.6	1
107	Using Ionâ€velocity Map Imaging Technique to Study Photodissociation of 2â€Bromopentane. Chinese Journal of Chemical Physics, 2013, 26, 493-497.	0.6	4
108	Laserâ€induced Fluorescence Spectroscopy of NiO between 510 and 650 nm. Chinese Journal of Chemical Physics, 2013, 26, 512-518.	0.6	2

#	Article	IF	CITATIONS
109	Laserâ€induced Fluorescence Spectroscopy of CoS: Identification of a New Excited State Arising from the Ground State. Chinese Journal of Chemical Physics, 2013, 26, 701-704.	0.6	3
110	Laserâ€induced Fluorescence Spectroscopy of NiS: Identification of a Lowâ€lying Electronic State. Chinese Journal of Chemical Physics, 2013, 26, 140-144.	0.6	1
111	Temperature Dependence of C ₂ (X ¹ Σ _g ⁺) in Reactions with Unsaturated Hydrocarbons. Wuli Huaxue Xuebao/ Acta Physico - Chimica Sinica, 2013, 29, 683-688.	2.2	0
112	Photodissociation of 2-Bromobutane at â^1⁄4265 nm by Ion-velocity Map Imaging Technique. Chinese Journal of Chemical Physics, 2012, 25, 373-378.	0.6	2
113	Note: Observation of a new electronically excited state of cobalt monoxide. Journal of Chemical Physics, 2012, 137, 206101.	1.2	2
114	Coherent Random Fiber Laser Based on Nanoparticles Scattering in the Extremely Weakly Scattering Regime. Physical Review Letters, 2012, 109, 253901.	2.9	108
115	Mode specific photodissociation of CS2+via the A2Îu state: a time-sliced velocity map imaging study. Physical Chemistry Chemical Physics, 2012, 14, 2468.	1.3	7
116	Laser-induced Fluorescence Spectroscopy of NiCl in 12900–15000 cmâ^'1. Chinese Journal of Chemical Physics, 2012, 25, 631-635.	0.6	2
117	Random fiber laser of POSS solution-filled hollow optical fiber by end pumping. Optics Communications, 2012, 285, 3967-3970.	1.0	31
118	Laser-launched evanescent surface plasmon polariton field utilized as a direct coherent pumping source to generate emitted nonlinear four-wave mixing radiation. Optics Express, 2011, 19, 4991.	1.7	3
119	Optical amplification of Eu(TTA)_3Phensolution-filled hollow optical fiber. Optics Letters, 2011, 36, 1902.	1.7	11
120	Phaseâ€locking of two independent degenerate coherent antiâ€Stokes Raman scattering processes: concept, proposed allâ€optical implementation, and potential applications. Journal of Raman Spectroscopy, 2011, 42, 1743-1746.	1.2	1
121	Photodissociation of 2-Bromobutane by Ion-velocity Map Imaging Technique. Chinese Journal of Chemical Physics, 2011, 24, 647-652.	0.6	8
122	Cavity Ringdown Spectroscopy of PH2 Radical in 465–555 nm. Chinese Journal of Chemical Physics, 2011, 24, 8-15.	0.6	1
123	Time-sliced Velocity Map Imaging Study on Photodissociation of Neopentyl Bromide and <i>Tert</i> -pentyl Bromide at 234 nm. Chinese Journal of Chemical Physics, 2011, 24, 631-634.	0.6	5
124	Multiphoton dissociative ionization of tert-pentyl bromide near 265 nm. Journal of Chemical Physics, 2011, 135, 244302.	1.2	10
125	Experimental Determination of the Vibrational Constants of FeS(<i>X</i> 5Δ) by Dispersed Fluorescence Spectroscopy. Chinese Journal of Chemical Physics, 2011, 24, 1-3.	0.6	7
126	[1 + 1] photodissociation of \${m CS}_{m 2}^ + (ilde X{}^{m 2}Pi _g)\$CS2+(XÌf2Îg) via the vibrationally mediated \$ilde B^{m 2} Sigma _u^ +\$BÌf2Ĩ£u+ state: Multichannels exhibiting and mode specific dynamics. Journal of Chemical Physics, 2011, 134, 114309.	1.2	12

#	Article	IF	CITATIONS
127	Note: Single-ultraviolet-photon dissociation dynamics of \${m CS}_{m 2}^ + (ilde X{}^2Pi _g)\$ CS 2+(Xìf2ìg) in 227–243 nm revealed by time-sliced velocity map imaging. Journal of Chemical Physics, 2011, 135, 116102.	1.2	3
128	Spectroscopy of nickel monosulfide in 450–560nm by laser-induced fluorescence and dispersed fluorescence techniques. Chemical Physics Letters, 2010, 493, 245-250.	1.2	6
129	Reactions of C2(a â^3u) with selected saturated alkanes: A temperature dependence study. Journal of Chemical Physics, 2010, 132, 164312.	1.2	8
130	Reaction of C2(a Î3u) with methanol: Temperature dependence and deuterium isotope effect. Journal of Chemical Physics, 2010, 133, 114306.	1.2	2
131	B-X and C-X Band Systems of CuCl Revisited: Laser-induced Fluorescence Study in 465–490 nm. Chinese Journal of Chemical Physics, 2010, 23, 249-251.	0.6	0
132	Laser-induced Fluorescence and Dispersed Fluorescence Spectroscopy of NiB: Identification of a New 2Î State in 19000–22100 cmâ^'1. Chinese Journal of Chemical Physics, 2010, 23, 626-629.	0.6	5
133	Laser-induced Fluorescence Spectrum of CoS Between 15200 and 19000 cmâ^'1. Chinese Journal of Chemical Physics, 2010, 23, 262-268.	0.6	4
134	Laser-induced atomic fragment fluorescence spectroscopy: A facile technique for molecular spectroscopy of spin-forbidden states. Review of Scientific Instruments, 2009, 80, 033111.	0.6	1
135	Laser-induced Fluorescence Excitation Spectrum of NiS in 1550017200 cm1. Chinese Journal of Chemical Physics, 2009, 22, 668-672.	0.6	4
136	Resonance-enhanced photon excitation spectroscopy of the even-parity autoionizing Rydberg states of Kr. Science in China Series B: Chemistry, 2009, 52, 161-168.	0.8	4
137	Laser-induced fluorescence spectroscopy of FeS in the visible region. Journal of Molecular Spectroscopy, 2009, 255, 101-105.	0.4	10
138	Absorption spectra of AsH2 radical in 435–510nm by cavity ringdown spectroscopy. Journal of Molecular Spectroscopy, 2009, 256, 192-197.	0.4	7
139	Photolysis of n-butyl nitrite and isoamyl nitrite at 355 nm: A time-resolved Fourier transform infrared emission spectroscopy and ab initio study. Journal of Chemical Physics, 2009, 130, 174314.	1.2	6
140	The laser-induced fluorescence study of A2Σâ^'–X2Îi band system of CuS. Journal of Molecular Spectroscopy, 2008, 252, 77-80.	0.4	7
141	In situ accurate determination of the zero time delay between two independent ultrashort laser pulses by observing the oscillation of an atomic excited wave packet. Optics Letters, 2008, 33, 1893.	1.7	2
142	On the photofragmentation of SF2+: Experimental evidence for a predissociation channel. Journal of Chemical Physics, 2008, 129, 166101.	1.2	0
143	Observation of the 5p Rydberg states of sulfur difluoride radical by resonance-enhanced multiphoton ionization spectroscopy. Journal of Chemical Physics, 2008, 128, 144306.	1.2	2
144	Resonance-Enhanced Photon Excitation Spectroscopy of the Even-Parity Autoionizing Rydberg States of Xe. Chinese Journal of Chemical Physics, 2008, 21, 401-406.	0.6	2

#	ARTICLE	IF	CITATIONS
145	Observation of above-threshold dissociation of amil:math xmlns:mml="http://www.w3.org/1998/Math/MathML" display="inline"> <mml:mmultiscripts><mml:mi mathvariant="normal">Na<mml:mn>2</mml:mn><mml:none></mml:none><mml:none /><mml:mo>+</mml:mo></mml:none </mml:mi </mml:mmultiscripts> in intense laser fields. Physical Review A,	1.0	5
146	Threshold ion-pair production spectroscopy of HCN. Journal of Chemical Physics, 2006, 124, 074310.	1.2	14
147	Coherent control and phase locking of two-photon processes in the nanosecond domain. Journal of the Optical Society of America B: Optical Physics, 2003, 20, 2255.	0.9	4
148	Study on the resonance-enhanced multiphoton ionization of the 4s and $\hat{Cl}f$ states of SF2 radicals. Journal of Electron Spectroscopy and Related Phenomena, 2000, 108, 135-139.	0.8	5
149	A new excited electronic state of SF2 radical observed by resonance-enhanced multiphoton ionization. Chemical Physics Letters, 1999, 305, 79-84.	1.2	10
150	Kinetic studies on state-state coupling and collisional quenching of excited sulfur dioxide. International Journal of Chemical Kinetics, 1998, 30, 831-837.	1.0	2
151	Electronic Band Systems of SF2 Radicals Observed by Resonance-Enhanced Multiphoton Ionization. Journal of Physical Chemistry A, 1998, 102, 7233-7240.	1.1	14
152	Resonance-enhanced multiphoton ionization spectroscopy of SF 2 radical. , 1998, , .		0
153	Soluble Hybrid Ionic Semiconductor and Its Photovoltaic Effect in Solution. ACS Applied Materials & Interfaces, 0, , .	4.0	2